Status and Challenges in the MQXFB Nb_3Sn quadrupoles for the HL-LHC

Susana Izquierdo Bermudez, Giorgio Ambrosio, Jerome Axensalva, Amalia Ballarino, Lucie Baudin, Christian Barth, Nicolas Bourcey, Thierry Boutboul, Delio Duarte Ramos, Arnaud Devred, Sandor Feher, Paolo Ferracin, Jose Ferradas Troitino, Lucio Fiscarelli, Jerome Fleiter, Ludovic Grand-Clement, Michael Guinchard, Simon Hopkins, Nicholas Lusa, Franco Mangiarotti, Attilio Milanese, Francois-Olivier Pincot, Rosario Principe, Mariano Pentella, Juan Carlos Perez, Carlo Petrone, Penelope Quassolo, Piotr Rogacki, Simon Staarup, Herve Prin, Stephan Russenschuck, Ezio Todesco, Gerard Willering.

***Abstract* - The inner triplet (or low-β) quadrupole magnets are among the components to be upgraded in LHC interaction regions for the HL-LHC project. The new quadrupole magnets, called MQXF, are based on Nb_3Sn superconducting magnet technology, with a conductor peak field of 11.3 T. CERN is in charge of the fabrication of the MQXFB variant, the longest Nb_3Sn accelerator magnets designed and manufactured up to now, with a magnetic length of 7.2 m. Two magnets, MQXFBP3 and MQXFB02, reached the HL-LHC project requirements. However, they still exhibited a limitation at 4.5 K with a phenomenology similar to the one observed on the first two prototypes. After improvements on the cold mass (longitudinal welding) and magnet assembly (elimination of overstress on the conductor during loading) procedures, a series of modifications were implemented in MQXFB03 at the level of the coil fabrication to address and/or reduce weaknesses in the coils. The magnet was tested and was the first to achieve performance requirements at both 1.9 K and 4.5 K, with no signs of conductor limitation at 4.5 K. MQXFB is now in the series production phase, with around 2/3 of the coils completed and half of the magnets assembled. We provide in this paper an overview of the MQXFB program, with a summary of the main recent achievements and an overall status of the fabrication.**

***Index Terms*—Nb_3Sn, Accelerator Magnets, HL-LHC**

I. Introduction

THE High Luminosity Upgrade of the Large Hadron Collider (HL-LHC) aims to boost the integrated luminosity by a factor of 10 [1]. Central to this upgrade are the triplet quadrupoles (Q1, Q2a, Q2b, Q3) [2]. The new magnets, called MQXF, will have a larger aperture (increasing from 70 mm to 150 mm), a higher peak field (from 8.6 T to 11.3 T), and will use Nb_3Sn superconducting material instead of Nb-Ti [3]. The Q1 and Q3 quadrupoles will have a magnetic length of 8.4 meters, divided into two 4.2-meter magnets (MQXFA) being produced by the US Accelerator Research Program (AUP) [4]. CERN is responsible for the 7.2-meter MQXFB magnets, which will be housed together with MCBXF corrector [5] for Q2a and Q2b cold masses. Both MQXFA and MQXFB share identical cross-sections and 3D design. The original design in 2013 targeted a gradient of 140 T/m for 7 TeV collision energy with a nominal current of 17.46 kA [3]. To enhance the operational margin, the magnetic length was extended early in the project from 6.80 meters to 7.15 meters. This modification allowed the required integrated gradient to be achieved with a reduced nominal current, thereby lowering the load line fraction (the ratio of operational current to maximum tolerable current) from 82% to 77% [6]. In 2020, based on feedback from magnetic measurements, the nominal reference current for the MQXF magnets was further reduced from 16.47 kA to

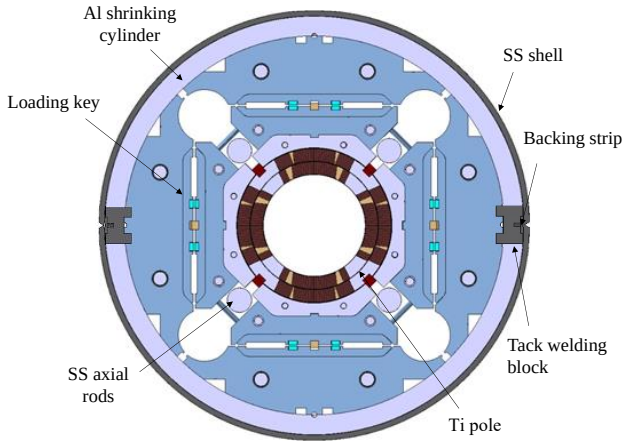

Fig. 1. MQXF magnet cross section

TABLE I. EVOLUTION OF MQXFB MAIN PARAMETERS FOR HL-LHC AT 7 TEV OPERATION PER BEAM

		2014 [6]	2015	2020 [7]
Nominal current	kA	17.46	16.47	16.23
Integrated Gradient	T	952.0	948.1	948.1
Gradient	T/m	140.0	132.6	132.2
Magnetic length	m	6.80	7.15	7.17
Load line fraction	%	82	77	76

Manuscript receipt and acceptance dates will be inserted here.
(Corresponding author: susana.izquierdo.bermudez@cern.ch*)*
Susana Izquierdo Bermudez, Giorgio Ambrosio, Jerome Axensalva, Amalia Ballarino, Lucie Baudin, Nicolas Bourcey, Thierry Boutboul, Delio Duarte Ramos, Arnaud Devred, Sandor Feher, Paolo Ferracin, Jose Ferradas Troitino, Lucio Fiscarelli, Jerome Fleiter, Ludovic Grand-Clement, Michael Guinchard, Simon Hopkins, Nicholas Lusa, Franco Mangiarotti, Attilio Milanese, Francois-Olivier Pincot, Rosario Principe, Mariano Pentella, Juan Carlos Perez, Carlo Petrone, Penelope Quassolo, Piotr Rogacki, Simon Staarup, Herve Prin, Stephan Russenschuck, Ezio Todesco, Gerard Willering are with CERN, CH-1211 Geneva 23, Switzerland.
Giorgio Ambrosio, Sandor Feher are with Fermi National Accelerator Laboratory (FNAL), Batavia, IL 60510 USA.
Paolo Ferracin is with Lawrence Berkeley National Laboratory (LBNL), Berkley, CA 94720 USA.
Color versions of one or more of the figures in this paper are available online at http://ieeexplore.ieee.org.
Digital Object Identifier will be inserted here upon acceptance.

16.23 kA, corresponding to a gradient of 132.2 T/m at 7 TeV collision energy [7]. Table I summarizes the evolution of the main magnetic parameters. The design and assembly of these magnets involves using water-pressurized bladders and keys to pre-stress the coil pack and pre-tension the aluminum shrinking cylinder at room temperature [8]. Once this is done, two 8-mm thick stainless steel half-shells are welded around the magnet to form a liquid helium containment vessel. This stainless shell (SS) and its contents are collectively referred to as the "cold mass". The cold mass assembly is completed by welding the end covers to the main cylinder made by the welded shells [9]. The cross-section of the cold mass is illustrated in Fig. 1.

A total of 10 MQXFB series magnets are needed for HL-LHC (8 to be installed and 2 spares). Up to date, six full length magnets have been manufactured and tested: MQXFBP1, MQXFBP2, MQXFBP3, MQXFB02, MQXFB03 and MQXFB04. Except MQXFB04, all magnets were first assembled and cryostated in a standalone configuration for faster assembly and test. From MQXFB04 onwards, MQXFB magnets are directly coupled with a corrector magnet in Q2a/b configuration. The next series magnet, MQXFB05, is now ready for testing, the cold mass containing the MQXFB06 magnet is prepared for welding, and assembly of the MQXFB07 magnet is underway.

The performance requirement for installation in HL-LHC is to reach (at 20 A/s) and hold nominal current (I_{nom} for 7 TeV operation, 16.23 kA) + 300 A at 1.9 K, the so-called I_{target} ($I_{target} = I_{nom} + 300$ A), with no specifications on the virgin training and up to 3 quenches to reach I_{nom} after a thermal cycle. Magnets are also tested at 4.5 K to the same current level, to probe the margin. In the machine, at nominal condition and in the most exposed regions, the coil temperature is expected to stay below 2.22 K [10]. The first two magnets, MQXFBP1 and MQXFBP2 were limited at 1.9 K at 93 % and 98 % of the nominal current. Following these results, a thorough root cause analysis was carried out and a 3-stage program was initiated to address the possible root causes [11]. The first stage addresses the mechanical coupling between the outer stainless-steel shell and the magnet structure, which was reduced to a minimal in MQXFBP3 [9]. The second stage addresses coil overstress during magnet loading, with a new assembly procedure applied in MQXFB02 [12]. Both magnets meet the HL-LHC requirements, in particular reaching 7 TeV equivalent current with a 300 A margin at 1.9 K, and no retraining after thermal cycles. However, they still show a limitation below target current at 4.5 K with a phenomenology similar to the one observed on MQXFBP1&2 thereby indicated that the root-cause of the problem had not been eradicated. Results were presented in [11][13][14]. The third stage of the program addresses the coil fabrication, implementing a series of modifications to reduce longitudinal, radial and azimuthal friction between coil and the reaction heat treatment fixture. Among the changes implemented the major ones are the partial compensation of the coil curing cavity aimed at reducing the azimuthal coil size prior to reaction and the removal of the ceramic binder from the outer layer of the coil [15]. MQXFB03, the first magnet assembled using new generation coils, is the

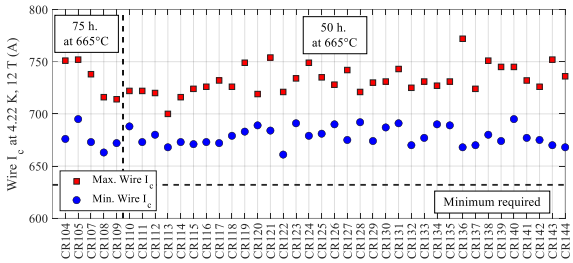

Fig. 2. Minimum and maximum strand critical current (12 T 4.22 K) based on strand witness samples reacted with the coil. The vertical line indicates the change of duration of the last plateau during reaction.

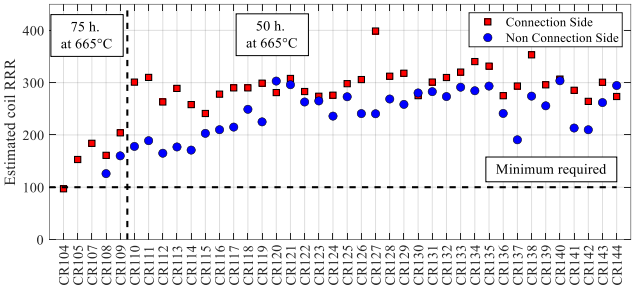

Fig. 3. Estimated coil RRR based on witness samples reacted with the coil. The vertical line indicates the change of duration of the last plateau during reaction

first 7.2-m-long Nb_3Sn accelerator magnet with no sign of conductor limitation at 4.5 K. A second magnet, MQXFB04, was built and tested using identical procedures, demonstrating the reproducibility of the technology. This paper provides an overall status of the fabrication and summarizes the main recent achievements in MQXFB program.

II. Status of The Fabrication

A. Conductor And Cable

MQXF coils are made with a Rutherford-type cable composed of 40 strands of 0.85 mm diameter and a copper to superconductor ratio of 1.2 ± 0.1. The requirements establish a minimum strand current of 632 A (331 A) at 12 T (15 T) and 4.2 K and a minimum Residual Resistivity Ratio (RRR) after cabling of 100. The cable incorporates a 12 mm wide 25 µm thick stainless-steel core to reduce inter-strand coupling currents. RRP® 108/127 strands from Bruker-OST will be used for all MQXFB series magnets. 90 % of the 2160 km of series wire procured by CERN has been received and accepted. In addition, 460 km of prototype/low performance wires was used as part of the prototyping program. At the end of 2022, CERN launched the procurement of 340 km of additional strand (10 MQXFB cable unit lengths) to have a strategic stock in case of need. The strand is expected to be delivered by 2025.

In total, 8 RRP ® 108/127 prototype cables and 54 series cables have been produced so far, with only two rejected cables (one rejected at the early stage of production due to a strand cross-over [16], one rejected more recently due to strand breakage following a sudden increase of the tension on a spool of the cabling machine). The 6 remaining cables to produce

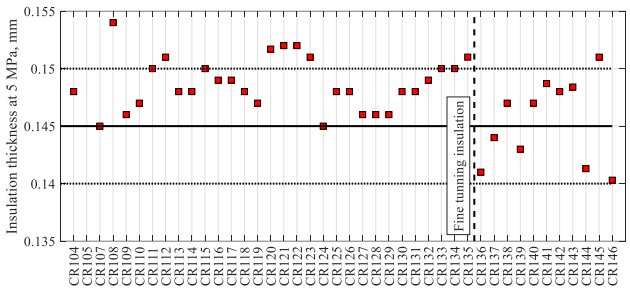

Fig. 4. Measured insulation thickness at 5 MPa.

the baseline number of coil will be completed early 2025. The MQXF coils are produced according to the wind, react and impregnate process. The reaction heat treatment process requires three 50 hours plateaus of 210 ºC, 400 ºC and 665 ºC. Only the coils of the first prototype magnet were reacted with a longer plateau at 665 ºC of 75 hours.

As can be seen in Fig. 2, the measured strand critical current for the units cabled so far is on average 10 % higher than initially specified, which translates to 3 % additional operation margin on the load line. The operation margin on the load line for the MQXFB coils assembled so far is 26-28 %. Except for the first coils, reacted with a 75-h plateau at 665 ºC, the RRR measured in witness samples reacted with the coil is also well above 100 (see Fig. 3). Samples are installed in both ends of the coils to monitor the cleanliness of the reaction process, since a significant degradation of the RRR in the non-connection side (outlet of the argon flow) was observed in the first coils [7].

The cable is insulated by directly braiding on two plies of 66 TEX S2 Glass filaments with 933 high temperature silane sizing. The target insulation thickness is 145 ± 5 µm at 5 MPa. Since the measured insulation was systematically above the target, a fine tuning of the insulation parameters was done in 2023 increasing the pitch length form 19 mm [17] to 21 mm. After the iteration, the cable thickness insulation is well centered around the 145 µm target (see Fig. 4).

B. *Coil Fabrication*

MQXF coil fabrication is based on the wind-and-react technology, where the superconducting phase is formed after winding and during coil heat treatment. The production of MQXFB coils started in 2016 with two copper coils followed by two low performance Nb_3Sn RRP conductor (CR001, CR002, CR101 and CR102) [18]. In spring 2017, the production of the coils for the first prototype started (CR104-CR109) [19]. Following a series of critical nonconformities (see Fig. 5, red bars), coil fabrication was put on hold for about six months in 2019 to enable review of manufacturing procedures and improvement of manufacturing process robustness. In September 2019 coil fabrication was resumed, with a production flow of approximately one coil per month [7]. In spring 2021, following the performance limitation observed on the first two prototype magnets, coil fabrication was stopped, while launching a root-cause analysis which included destructive inspections on selected coils [11]. As explained in the introduction, a series of modifications were implemented in the coil manufacturing process in a systematic manner [15]. Since the re-start of the coil production in September 2022, 21 coils have been completed and 3 coils are in fabrication (see Fig. 5). To complete the baseline number of coils, 18 more coils need to be wound. Coil yield is excellent, since the original baseline for the project assumed the construction of five coils per quadrupole, but in the last 2 years there has not been any critical nonconformity leading to coil rejection.

C. *Magnet and Cold mass assembly*

Assembly of MQXF magnets relies on a system of water-pressurized bladders and keys to pre-compress the coils and to pre-tension the aluminum cylinder during loading at room temperature (RT). The assembly of the MQXF structure is described in detail in [20]-[27]. Table II summarizes the maximum measured stress in the coil and the aluminium shell during bladder pressurization and the average stress after loading. Thanks to the use of auxiliary bladders in the yoke [12], implemented from MQXFB02, the peak stress in the coil has been significantly reduced and stays below 100 MPa (see Table II), which has been set as a conservative limit to prevent the occurrence of cracks in the Nb_3Sn phase [28].

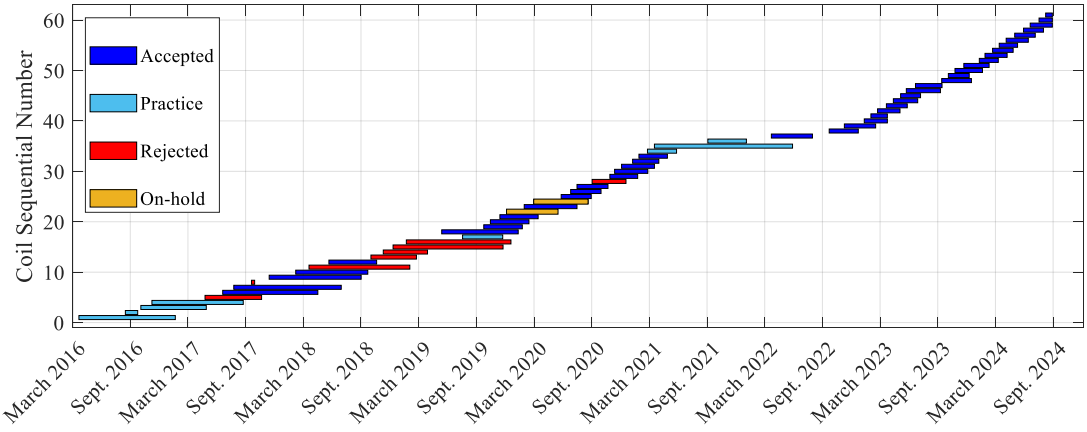

Fig. 5. MQXFB coil production dashboard.

TABLE II. AZIMUTHAL STRESS [MPA] IN THE COIL POLE AND ALUMINUM SHELL DURING ROOM TEMPERATURE LOADING

	Peak during bladder pressurization		Average after key insertion	
	Pole	Al-Shell	Pole	Al-Shell
MQXFBP1	-151	96	-87	72
MQXFBP2	-138	86	-86	54
MQXFBP3	-138	82	-75	46
MQXFB02	-45	142	-63	56
MQXFB03	-87	128	-81	48
MQXFB04	-92	154	-91	54
MQXFB05	-64	145	-94	53
MQXFB06	-86	145	-89	52

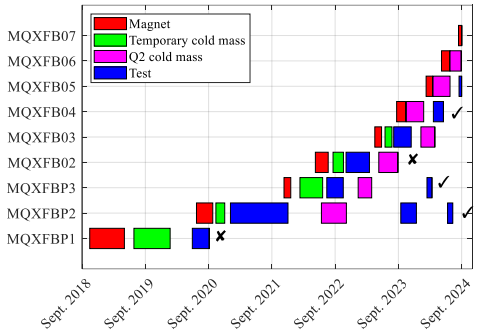

Fig. 6. MQXFB magnet dashboard.

Upon loading completion, the magnet is enclosed by a vacuum-tight stainless-steel shell for helium containment. Initially, prototypes and first-series magnets were assembled in temporary cold masses and cryostats to expedite turnaround times and test station availability, with full commissioning to test Q2 cold masses in their final configuration achieved in May 2023. Four temporary cryostat and cold mass assemblies had to be disassembled to recover the quadrupole magnets, which were then reassembled with an MCBXF corrector in a Q2 cold mass and cryostat. Also, a significant effort was undertaken to upgrade the CERN cryogenic test station, initially designed to test LHC magnets, but which had to be adapted to accommodate HL-LHC magnets having different height and He piping configuration.

The first two Q2 cold masses, containing MQXFBP2 and MQXFBP3 magnets, have been qualified for installation in the HL-LHC string [29]. During the reassembly of MQXFB02 in a Q2 cold mass, a 3.7 kV heater-to-coil high voltage test was conducted, despite the MQXF magnets' electrical design criteria stipulating a maximum applicable voltage of 460 V after helium exposure, due to potential damage from high voltage testing in air-helium mixture conditions at room temperature [30]. One of the heaters failed under these non-conforming testing conditions, necessitating the magnet's disassembly. The Q2 cold masses containing the MQXFB03 and MQXFB05 magnets are prepared for testing, and the first fully qualified Q2 cryo-assembly containing the MQXFB04 magnet is ready for final preparation before installation in the HL-LHC, marking a significant milestone for the project. Figure 6 illustrates the timeline.

III. TEST RESULTS

A. Magnet Performance

MQXFB prototype magnets BP1 and BP2 were limited to 94% and 98% of the current required for 7 TeV operation at 1.9 K. The subsequent magnets, MQXFBP3 and MQXFB02, with improved cold mass and magnet assembly procedures, met HL-LHC requirements, achieving a 7 TeV equivalent current with a 300 A margin and no retraining after thermal cycles, but still showed limitations at 4.5 K. Results were extensively presented [13][14]. As discussed in the introduction, a series of modifications were implemented at the level of the coil to address the performance limitations [15]. Two magnets were built and tested so far using all recovery actions from the 3 stages of the recovery program. Here the focus is the results from the last year: two virgin magnets (B03 and B04) and two Q2 cryo-assemblies containing the already tested prototype magnets (BP2 and BP3).

MQXFB03 reached nominal current (16.23 kA) after five training quenches at the nominal ramp of 20 A/s, and the target current (16.53 kA) after eight training quenches (see Fig. 7). The training quench location at 1.9 K is quite different from previous MQXFB magnets: in this magnet, all but the first quench are located in the coil heads; while for previous magnets the quenches were located in the straight section. Ex-

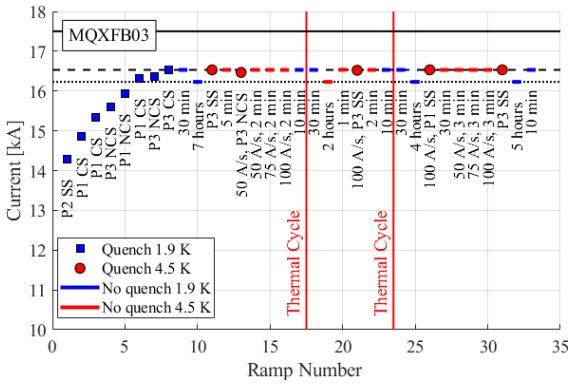

Fig. 7. MQXFB03 quench history. If not specified, current is ramped at the nominal rate of 20 A/s. Labels indicate quench location (pole and longitudinal position, SS: straight section, NCS: nonconnection side, CS: connection side).

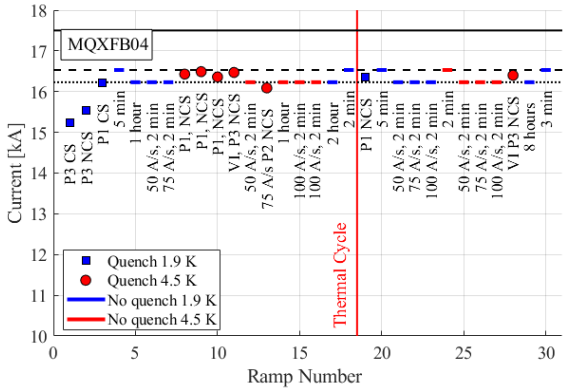

Fig. 8. MQXFB04 quench history. If not specified, current is ramped at the nominal rate of 20 A/s. Labels indicate quench location (pole and longitudinal position, SS: straight section, NCS: nonconnection side, CS: connection side).

cept for the first quench, only the coils in quadrant 1 and 3 quenched, consistent with the findings in MQXFA that coils that coils which were subjected to "overcurrent" due to the Coupling Loss Induced Quench (CLIQ) [31] protection system did not train [32]. Successive ramps at 1.9 K at the nominal ramp rate (20 A/s) did not provoke a quench up to the target current. The magnet also reached target current at 4.5 K and ramp rates up to 100 A/s, showing a significant improvement with respect to previous magnets, which all showed performance limitation and ramp rate sensitivity. Voltage-current (VI) cycles did not show a voltage buildup in the coils, within the measurement system precision. The magnet reached target current after thermal cycle without quench, showing excellent memory.

MQXFB04 reached the target current of 16.53 kA after three training at 1.9 K (see Figure 8). The training pattern was similar to that of MQXFB03, with quenches occurring near the coil ends in the first and third quadrants. Following the training at 1.9 K, the magnet successfully maintained the target current for 5 minutes and the nominal current for 1 hour at 1.9 K. It also reached the nominal current at higher ramp rates of 50 and 75 A/s at 1.9 K. At 4.5 K, the magnet experienced four quenches close to the target current. These quenches, which are localized in the coil head, were considered as training quenches. Subsequently, the magnet was able to sustain the nominal current for 1 hour and to achieve nominal current

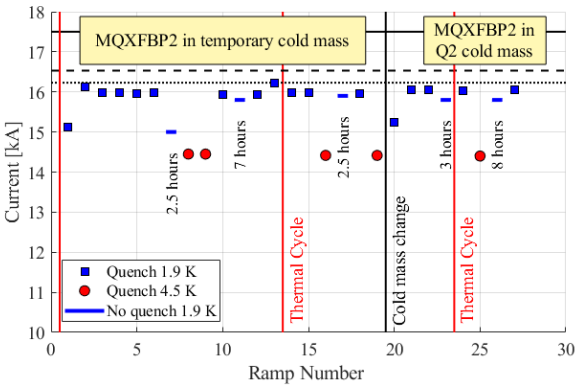

Fig. 9. MQXFBP2 quench history, assembled first in a temporary cold mass and then in a Q2 final cold mass. Only ramps at 20 A/s, all quenches were in the straight section of pole 1.

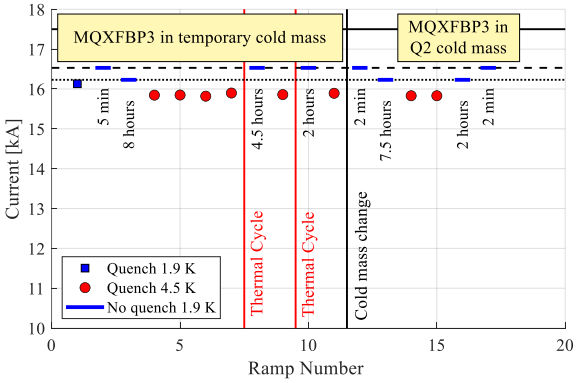

Fig. 10. MQXFBP3 quench history, assembled first in a temporary cold mass and then in a Q2 final cold mass. Only ramps at 20 A/s, all quenches except the first one were in the straight section of pole 4.

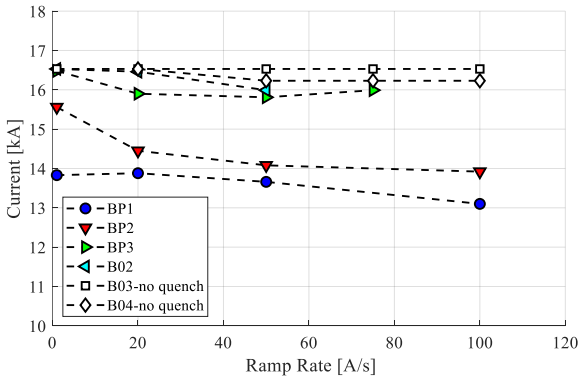

Fig. 11. Ramp rate studies at 4.5 K in MQXFB magnets. Empty markers indicate that the current is reached without a quench

with a ramp rate of 100 A/s without quenching. After a thermal cycle, the magnet reached the target current at 1.9 K after one training quench and at 4.5 K with no additional training quench. At the end of the test campaign, the magnet was able to maintain the nominal current for 8 hours at 1.9 K. Two voltage-current (VI) cycles [33] were performed to detect any indications of superconductor limitations when approaching the critical surface, showing no measurable resistive transition in the conductor. Additionally, several ramps were conducted to measure the field, with the magnet operating for a total of 28 hours operating at nominal current or above.

Two more cryo-assemblies containing the previously tested magnets MQXBP2 and MQXFBP3 were evaluated in the past twelve months. In both cases, the power performance of the magnets was consistent with previous tests, in particular with a good repeatability in the level of performance limitation, with no degradation. This demonstrates that full disassembly and reassembly of the cold mass do not impact magnet performance. MQXFBP3 successfully sustained the current of 16.23 kA for 8 hours at 1.9 K, while for MQXFBP2, the 8-hour holding current test was conducted at 15.8 kA to avoid a natural quench due to conductor limitations. Figures 11 and 12 illustrate the powering history, including only the ramps at the nominal ramp rate of 20 A/s. Higher ramp rate tests were also systematically conducted. Figure 11 summarizes the maximum current reached at 4.5 K as a function of the ramp rate for all the magnets tested so far. MQXFB03 and MQXFB04 did not quench up to the maximum current tested at 100 A/s, whereas MQXFBP2 was limited to 13.9 kA at 100 A/s and MQXFBP3 at 16 kA at 75 A/s.

B. Endurance

An endurance campaign was performed on MQXFB02, including 4 cool downs from room temperature to cryogenic temperature, 36 quenches at nominal current or above, and more than 500 current cycles up to nominal current or above. The magnet performance appears repeatable, including the limitation at 4.5 K, confirming that the cycling did not result in performance degradation. None of the MQXFB magnets tested to date have shown any degradation in performance following thermal or current cycling. All magnets successfully operated at the maximum achieved current without experienc-

TABLE III. SUMMARY ON THE NUMBER OF CYCLES, QUENCHES AND HOURS OPERATING AT OR ABOVE NOMINAL CURRENT IN MQXFB MAGNETS.

	# Thermal Cycles	# Cycles to $I \geq I_{nom}$	# Quenches at $I \geq I_{nom}$	Hours at $\geq I_{nom}$
BP1	2	0	0	0
BP2	5	17	7	14
BP3	4	70	10	44
B02	4	508	36	38
B03	3	50	18	24
B04	2	44	7	28
Total	20	1378	156	298

ing flattop quenches. Table III summarizes, for each magnet, the number of thermal and current cycles, the number of quenches at currents above the nominal level, and the total operating hours at or above the nominal current.

C. Magnetic Measurements

Specific instruments, together with a comprehensive strategy, have been developed for the magnetic measurements both at ambient and cryogenic temperatures [34]. The results of the magnetic characterization of eight magnets show that the transfer function, defined as the ratio between the integrated gradient and the current, is reproducible from magnet to magnet within 20 units of 10^{-4}, as summarized in Table IV. The field quality, after magnetic shimming, is under control and all multipoles are well within the required range of variation, as shown in Fig. 6.

D. Electrical Integrity

Electrical integrity is important for machine operation. Two critical non-conformities were recently identified during cold powering test. The first issue, located in the Q2 cryo-assembly containing the MQXFBP2 magnet, was a short circuit between the main circuit and ground at the level of the cold mass end-covers. This fault was repaired without disassembling the cryostated cold mass, as removing the cold bore was sufficient to address the damage. The assembly was subsequently retested to validate the repair, and the design was modified to prevent similar issues in the future.

The second non-conformity was an electrical weakness between the heater and the coil. Coil-to-heater high-voltage tests are conducted in air at 300 K after fabrication, in liquid helium (He) at 1.9 K, and again at 300 K after He exposure. In 2019, an additional conservative test at 100 K in 1.3 bar He gas was introduced to ensure margin after training and thermal cycling, applying 850 V [35]. One of the heaters in MQXFBP3 failed this test. Consequently, the heater was disconnected, and the assembly will be used as is for the HL-LHC string, as the protection system provides sufficient redundancy to operate with up to two quench heater circuit missing. The test procedure was modified to limit the risk of damage in future magnets, keeping the same test voltage and conditions (850 V, 100 ± 20 K and 1.3 ± 0.2 bar).

TABLE IV. TRANSFER FUNCTION MEASURED IN MQXFB MAGNETS

	Transfer function (T kA^{-1})	
	300 K	1.9 K at I_{nom}
MQXFBP1	63.394	58.562
MQXFBP2	63.359	58.708
MQXFBP3	63.328	58.616
MQXFB02	63.407	58.649
MQXFB03	63.458	58.571
MQXFB04	63.426	58.654
MQXFB05	63.434	–
MQXFB06	63.396	–
Average	64.000	58.627
Range (units)	20	25

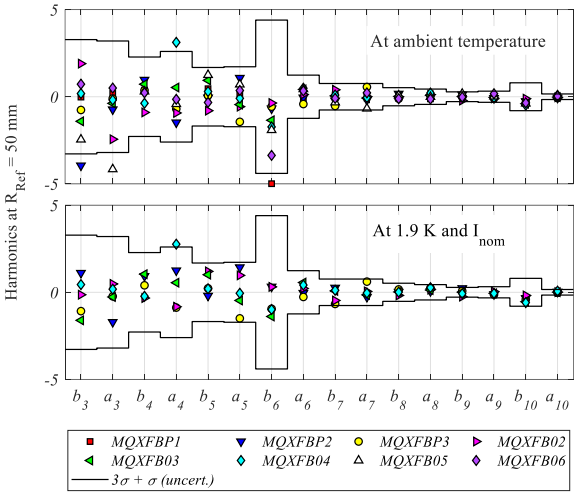

Fig. 6. multipoles measured on the prototypes and first series MQXFB quadrupoles. The solid lines show the expected range of random variation computed from random movements of 30 μm of the conductor blocks in the coils. The reference radius is 50 mm.

IV. CONCLUSIONS

MQXFB program has made significant progress in the development of Nb_3Sn superconducting quadrupole magnets for the High Luminosity LHC. The successful resolution of key technical challenges, particularly in coil fabrication and scaling up the technology to produce 7.2-meter-long accelerator-quality magnets, marks a significant milestone. The program has now advanced into the series production phase. The consistent performance of the most recent magnets, MQXFB03 and MQXFB04, particularly their ability to operate at the nominal current at both 1.9 K and 4.5 K, demonstrates the effectiveness of the modifications introduced. As the program continues, the focus will remain on maintaining the high quality of production and ensuring that the remaining magnets meet the HL-LHC's rigorous operational standards paving the way for enhanced performance in future collider operations.

ACKNOWLEDGMENTS

The authors wish to thank the CERN TE-MSC technical staff for the construction and cold powering tests of the magnets and for the strong and continuous support of the CERN TE and HL-LHC project managements.

REFERENCES

[1] O. Bruning et al, “LHC design report” Vol. 1, CERN 2004-003.

[2] E Todesco *et al* 2021 *Supercond. Sci. Technol.* 34 053001

[3] P. Ferracin et al., “Magnet design of the 150 mm aperture low-β quadrupoles for the high luminosity LHC,” *IEEE Trans. Appl. Supercond*., vol. 24, no. 3, Jun. 2014, Art. no. 4002306.

[4] G. Ambrosio, et al., “Lessons learned from the prototypes of the MQXFA Low Beta Quadrupoles for HL-LHC and plans for production in the US,” *IEEE Trans. Appl. Supercond.*, submitted for publication.

[5] J. A. García-Matos et al., "Fine Tuning of the Inner Dipole Design of MCBXF Magnets," in IEEE Transactions on Applied Superconductivity, vol. 32, no. 6, pp. 1-5, Sept. 2022, Art no. 4000405, doi: 10.1109/TASC.2022.3148688.

[6] S. Izquierdo Bermudez et al., "Second-Generation Coil Design of the Nb_3Sn low-β Quadrupole for the High Luminosity LHC," in IEEE Transactions on Applied Superconductivity, vol. 26, no. 4, pp. 1-5, June 2016, Art no. 4001105, doi: 10.1109/TASC.2016.2519002.

[7] S. I. Bermudez et al., "Progress in the Development of the Nb3Sn MQXFB Quadrupole for the HiLumi Upgrade of the LHC," in *IEEE Transactions on Applied Superconductivity*, vol. 31, no. 5, pp. 1-7, Aug. 2021, Art no. 4002007, doi: 10.1109/TASC.2021.3061352.

[8] S. Caspi, et al., “The use of pressurized bladder for stress control of superconducting magnets,” *IEEE Trans. Appl. Supercond*. 11 (2001) 2272-2275

[9] H. Prin et al., "First CERN Cold Masses for the HL-LHC Interaction Regions," in IEEE Transactions on Applied Superconductivity, vol. 34, no. 5, pp. 1-5, Aug. 2024, Art no. 4004805, doi: 10.1109/TASC.2024.3364134.

[10] P. Borges de Sousa et al., "Numerical Assessment of the Inhomogeneous Temperature Field and the Quality of Heat Extraction of Nb3Sn Impregnated Magnets for the High Luminosity Upgrade of the LHC," in IEEE Transactions on Applied Superconductivity, vol. 33, no. 5, pp. 1-5, Aug. 2023, Art no. 4000705, doi: 10.1109/TASC.2023.3240126.

[11] S. I. Bermudez et al., "Status of the MQXFB Nb3Sn Quadrupoles for the HL-LHC," in IEEE Transactions on Applied Superconductivity, vol. 33, no. 5, pp. 1-9, Aug. 2023, Art no. 4001209, doi: 10.1109/TASC.2023.3237503.

[12] J. Ferradas Troitino et al., "Optimizing the use of pressurized bladders of the assembly of superconducting magnets: the HL-LHC MQXFB quadrupole magnet case," 2023 *Supercond. Sci. Technol.* **36** 065002

[13] E. Todesco et al., "Status and Challenges of the Interaction Region Magnets for HL-LHC," in IEEE Transactions on Applied Superconductivity, vol. 33, no. 5, pp. 1-8, Aug. 2023, Art no. 4001608, doi: 10.1109/TASC.2023.3244143.

[14] A. Milanese et al., "Status of MQXFB Quadrupole Magnets for HL-LHC", JACoW IPAC2023 (2023) WEPM060 DOI: 10.18429/JACoW-IPAC2023-WEPM060.

[15] N. Lusa et al., "Towards MQXFB Series Coils," in IEEE Transactions on Applied Superconductivity, vol. 34, no. 5, pp. 1-8, Aug. 2024, Art no. 4003408, doi: 10.1109/TASC.2024.3360928.

[16] J. Fleiter, S. Peggiani, A. Bonasia and A. Ballarino, "Characterization of Nb3Sn Rutherford Cable Degradation Due to Strands Cross-Over," in IEEE Transactions on Applied Superconductivity, vol. 28, no. 4, pp. 1-5, June 2018, Art no. 4802205, doi: 10.1109/TASC.2018.2809474.

[17] E. F. Holik et al., "Fabrication and Analysis of 150-mm-Aperture Nb3Sn MQXF Coils," in IEEE Transactions on Applied Superconductivity, vol. 26, no. 4, pp. 1-7, June 2016, Art no. 4000907, doi: 10.1109/TASC.2015.2514193.

[18] F. Lackner *et al.*, “Status of the Long MQXFB Nb_3Sn coil prototype production for the HiLumi LHC,” *IEEE Trans. Appl. Supercond.*, vol. 27, no. 4, Jun. 2017, Art. no. 4002605.

[19] F. Lackner et al., "Fabrication of the 7.3-m-Long Coils for the Prototype of MQXFB, the Nb3Sn Low-b Quadrupole Magnet for the HiLumi LHC," in IEEE Transactions on Applied Superconductivity, vol. 28, no. 3, pp. 1-5, April 2018, Art no. 4005605, doi: 10.1109/TASC.2018.2792466.

[20] E Takala *et al* 2021 *Supercond. Sci. Technol.* 34 095002

[21] G. Vallone et al., “Mechanical performance of short models for MQXF, the Nb3 Sn low-β quadrupole for the hi-lumi LHC,” IEEE Trans. Appl. Supercond., vol. 27, no. 4, Jun. 2017, Art. no. 4002906.

[22] H. Pang et al., “Mechanical design studies of the MQXF long model quadrupole for the HiLumi LHC,” IEEE Trans. Appl. Supercond., vol. 27, no. 4, Jun. 2017, Art. no. 4004105.

[23] G. Vallone et al., “Mechanical design analysis of MQXFB, the 7.2-m-long low-β quadrupole for the high-luminosity LHC upgrade,” IEEE Trans. Appl. Supercond., vol. 28, no. 3, Apr. 2018, Art. no. 4003705.

[24] G. Vallone et al., “ Assembly of MQXFBP1, mechanical model of the 7.2 m long low-β quadrupole for the high luminosity LHC upgrade,” IEEE Trans. Appl. Supercond., to be published.

[25] G. Vallone et al., “Mechanical analysis of the short model magnets for the Nb3 Sn low-β quadrupole MQXF,” IEEE Trans. Appl. Supercond., vol. 28, no. 3, Apr. 2018, Art. no. 4003106.

[26] G. Vallone et al., “Summary of the mechanical performances of the 1.5 long models of the Nb3Sn low-β quadrupole MQXF,” IEEE Trans. Appl. Supercond., vol. 29, no. 9, Aug. 2019, Art. no. 4002805.

[27] E. Takala et al., “On the mechanics of MQXFB - the low beta quadrupole for the HL-LHC,” 2021 *Supercond. Sci. Technol.* 34 095002

[28] K. Puthran et al., "Onset of Mechanical Degradation due to Transverse Compressive Stress in Nb^3Sn Rutherford-Type Cables," in IEEE Transactions on Applied Superconductivity, vol. 33, no. 5, pp. 1-6, Aug. 2023, Art no. 8400406, doi: 10.1109/TASC.2023.3241568.

[29] M. Bajko et al., “Transforming Concept into Reality: Overcoming Vhallenges in the HL-LHC IT STRING Test Stand Implementation”, in IEEE Transactions on Applied Superconductivity, ASC2024

[30] V. Marinozzi et al., "Study of the Heater-Coil Electrical Insulation for the HL-LHC Low Beta Quadrupoles," in IEEE Transactions on Applied Superconductivity, vol. 31, no. 5, pp. 1-5, Aug. 2021, Art no. 4001705, doi: 10.1109/TASC.2021.3061348.

[31] E. Ravaioli, “CLIQ. A new quench protection technology for superconducting magnets”, PhD : Twente U., Enschede : 2015

[32] S. Stoynev et al., "Effect of CLIQ on Training of HL-LHC Quadrupole Magnets," in IEEE Transactions on Applied Superconductivity, vol. 34, no. 5, pp. 1-6, Aug. 2024, Art no. 4900606, doi: 10.1109/TASC.2023.3341871.

[33] R. Keijzer et al., “Modelling V-I Measurements of Nb3Sn Accelerator Magnets with Conductor Degradation,” IEEE Trans. Appl. Supercond., v. 32, n. 6, Sept. 2022

[34] L. Fiscarelli et al., " Measurement of integrated gradient and field quality on the first Q2 magnets for HL-LHC", JACoW IPAC2024 (2024) DOI: 10.18429/JACoW-IPAC2024

[35] M. Baldini et al., "Assessment of MQXF Quench Heater Insulation Strength and Test of Modified Design," in IEEE Transactions on Applied Superconductivity, vol. 31, no. 5, pp. 1-5, Aug. 2021, Art no. 4701305, doi: 10.1109/TASC.2021.3058223.